Modeling and parameter estimation of a catalyst deactivation fluidized bed reactor

Simira Papadopoulou, Georgia Kokolaki
and Ismini Anastasiou
Technological Educational Institute of Thessaloniki
Thessaloniki 541 01, Greece
shmira@teithe.gr

Spyros Voutetakis and Panos Seferlis
Chemical Process Engineering Research Institute/CERTH
Thermi-Thessaloniki 570 01, Greece
{paris, seferlis}@cperi.certh.gr

***Abstract* - The aim of the present work is the development of a detailed dynamic mathematical model of a fluidized bed reactor with distributed parameters, in radial and axial direction, which will form the basis of a model predictive controller. A set of partial differential equations describes the dynamic behavior of the conductive and convective heat transfer. The model is divided in five sections in accordance to the heating sections of the reactor. In each section the model contains six different sub models corresponding to the six different layers that make up the reactor in the radial direction. The model validation and the parameter estimation were performed using dynamic experimental data from the unit at different operating conditions. Optimal estimates for key parameters were calculated using the Maximum Likelihood method. The obtained results revealed the ability of the model to predict accurately the operation of the reactor unit.**

Index terms – Modeling, parameter estimation, catalyst deactivation, Model Predictive Control, fluidized bed reactor.

I. INTRODUCTION

The FCC process is a vital part of every modern refinery. Through this process the heavy residue of the atmospheric and vacuum distillations is catalytically converted from heavy to lighter hydrocarbon products thus increasing the gasoline and diesel yield of the refinery. In order to evaluate the performance of FCC catalysts in bench scale units and pilot plants one must have pre-processed samples from the fresh vendor supplied catalysts that accurately simulate the state of a "used" catalyst that actually is present at any given time inside the commercial FCC unit. Such a unit is the cyclic propylene deactivation pilot plant unit of CPERI / CERTH which is a fluidized bed reactor. The operation of the cyclic propylene steam deactivation unit (CPS) that guarantees the preparation of catalysts with predefined quality strongly depends on the tight control of temperature in the reactor. Temperature control of the unit is quite challenging for the following reasons:

- The temperature during heat-up should follow a predefined ramping profile with 3 steps to the final level of 780 ºC.
- Large time delays are involved, that also change over the operational range and therefore the control system must be tuned accordingly. This is generated by cycling the feeds (20 times) from oxidizing to neutral and reducing environment.
- At the final stage of the ramp, the temperature overshoot should not exceed 2%, in order to avoid damage to the catalyst and to ensure the catalyst's final properties.

The complexity of the control objectives and the multiple cycles of operation make the use of an optimal model predictive control (MPC), a viable candidate.

In order to develop a reliable optimal MPC system (Fig.1) [1], a mathematical model is necessary for the prediction of the future dynamic effects of the control actions in the distributed process. Dynamic measurement data from the unit provide the necessary information for the correction of the model predictions through the calculation of optimal estimates for key model parameters.

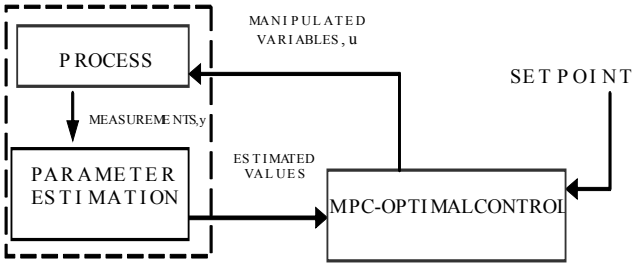

Fig. 1 Optimal MPC control

II. DESCRIPTION OF THE UNIT

The flow diagram of the cyclic propylene steam deactivation procedure used to prepare (FCC) catalysts for performance evaluation is shown in Fig. 2. The catalyst processing takes place in a cylindrical fluidized bed reactor, which is heated by four electric resistances, placed in refractory insulation material around the reactor surface.

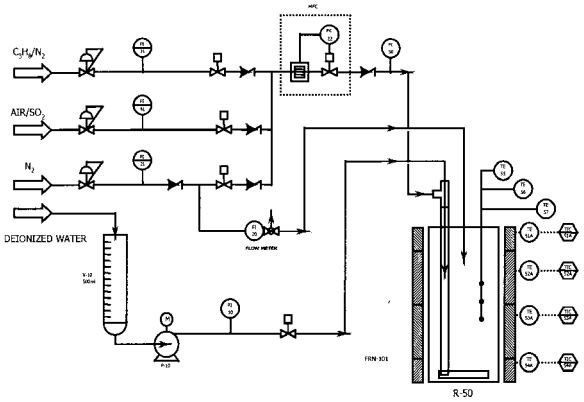

Fig. 2 Simplified diagram of the CPS unit

The whole reactor is covered with insulated material for the reduction of thermal losses.

The process of deactivation includes alternating stages of reduction and oxidation with corresponding endothermic and exothermic reactions. The reduction and coke deposition is achieved via a gas stream that contains steam and propylene, while the oxidation and coke combustion is achieved via the feed of an air/sulphur mixture and a steam stream. After the loading of catalyst in the reactor, the furnace is heated gradually in predefined steps (ramp) until it reaches the final desirable operating temperature (780 ºC). Between the stages the unit is supplied with nitrogen.

The catalyst is impregnated with metals (i.e. vanadium or nickel from a source such as metal naphthenates) before steaming. The deactivation of catalysts is achieved with hydrothermal deactivation combined with chemical cracking. The steaming process is designed to hydrothermally cracking catalysts and to simultaneously deactivate metals deposited on the catalyst. The process' temperature must be closely monitored and the heat up must be carried out in a predefined and consistent way. Even relatively small overshoots in the final temperature might give to the processed catalysts properties that are not acceptable. At the end of the deactivation procedure that lasts more than 22 hours in total, the catalyst must have the exact macroscopic properties that match the catalyst drawn from the industrial process. The whole process needs to be accurate and repeatable in the higher extend possible.

III. MODELING

The CPS process model considers heat transfer in the radial and the axial direction, through the mechanisms of conduction and convection. The structure of the unit comprises successive layers in the radial direction as shown in Fig. 3.

From inside to outside:

- The catalyst bed at the interior of the reactor where the reactions take place (CATALYST, INTAIR).
- The reactor wall made of alloy steel (TUBE).
- The intermediate air gap (MAIR).
- The resistance, which is embedded in refractory material and is considered the heating surface (HEATER).
- The insulator made of refractory material in order to withstand high temperatures and to prevent heat losses (INS).
- The outer wall made of a thin sheet of stainless steel (WALL).

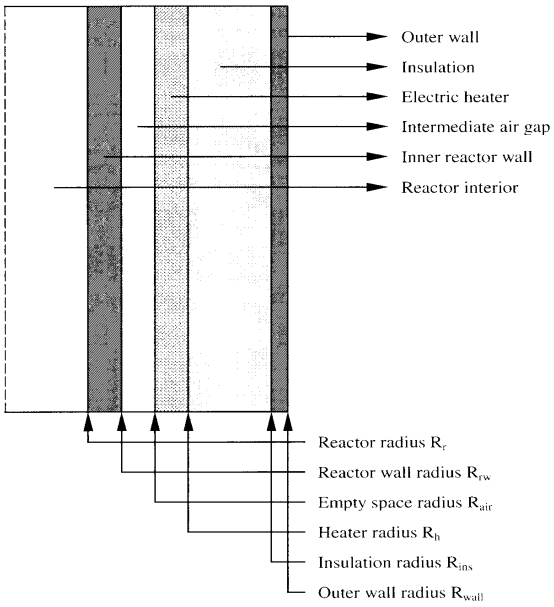

Fig.3 Schematic of a vertical cross-section of the cylindrical furnace reactor

Electric resistances embedded in refractory material in the heater section generate the necessary heat for the process. Heat is then transported in the radial direction towards the center of the reactor and outwards through the insulator and in the axial direction towards the lower and upper sections. A distributed heat transfer model is in two dimensions (r, z) developed for the different layers that consist the unit. The dynamic behavior of the temperature is hence expressed as a set of partial differential equations.

The mathematical model simulates a semi-batch procedure with great changes of temperature (200-780 ºC), as the dynamic behavior of the system changes, due to the cyclic variations of operating conditions from endothermic to exothermic. The model is divided in 5 sections in the axial direction of the reactor, in accordance with the five heating zones (Fig. 4).

Heat transfer through conduction and convection was taken into account in each section. The initial values of the parameters (material conductivities, heat transfer coefficients, material densities etc.) were chosen from

literature taking into consideration the operating conditions and the materials of construction of the unit. The catalyst is placed in the inner part of the reactor corresponding to the third section. The model considers the catalyst as a pseudo-homogenous fluidized bed. Heat transfer through convection [2] due to the flow of the gases through the reactor is considered in the inner part of the reactor, in the three upper sections. The model equations for the third section (Fig. 4) are:

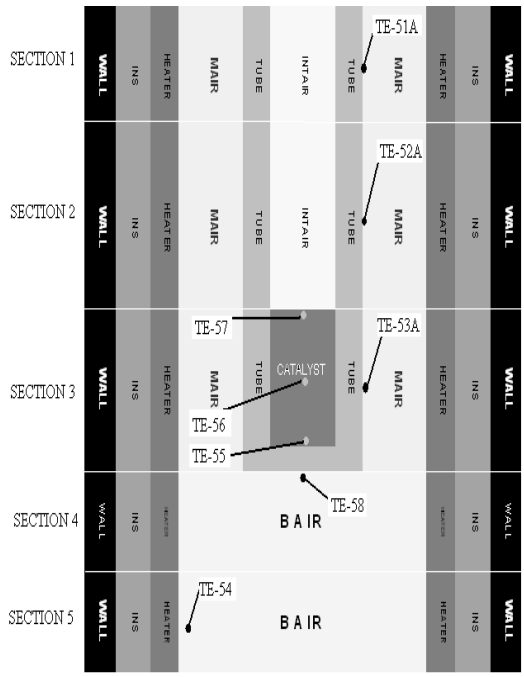

Fig.4 Schematic representation of the mathematical model and the position of the measurement points of the unit

For the catalyst:

$$(\rho Cp)_{cat}\frac{\partial T}{\partial t}+(\rho Cp)_{cat}U_z\frac{\partial T}{\partial z}=k_{cat}\left[\frac{\partial^2 T}{\partial z^2}+\frac{1}{r}\left(\frac{\partial}{\partial r}\left(r\frac{\partial T}{\partial r}\right)\right)\right] \quad (1)$$

Boundary conditions:

$$-k_{cat}\left.\frac{\partial T}{\partial z}\right|_{z=L_a}=h_l\left[T(L_a,r)-T_l(r)\right] \qquad \text{For z =}L_a\ (1.1)$$

$$-k_{cat}\left.\frac{\partial T}{\partial z}\right|_{z=L_b}=h_u\left[T_u(r)-T(L_b,r)\right] \qquad \text{For z =}L_b\ (1.2)$$

$$-k_{cat}\left.\frac{\partial T}{\partial r}\right|_{r=R_a}=0 \qquad \text{For r =}R_a\ (1.3)$$

$$-k_{cat}\left.\frac{\partial T}{\partial r}\right|_{r=R_b}=h_{cat}\left[T(z,R_b)-T_b(z)\right] \qquad \text{For r =}R_b\ (1.4)$$

For the reactor wall:

$$(\rho Cp)_{tube}\frac{\partial T}{\partial t}=k_{tube}\left[\frac{\partial^2 T}{\partial z^2}+\frac{1}{r}\left(\frac{\partial}{\partial r}\left(r\frac{\partial T}{\partial r}\right)\right)\right] \quad (2)$$

Boundary conditions:

$$-k_{tube}\left.\frac{\partial T}{\partial z}\right|_{z=L_a}=h_l[T(L_a,r)-T_l(r)] \qquad \text{For z =}L_a\ (2.1)$$

$$-k_{tube}\left.\frac{\partial T}{\partial z}\right|_{z=L_b}=h_u[T_u(r)-T(L_b,r)] \qquad \text{For z =}L_b\ (2.2)$$

$$-k_{tube}\left.\frac{\partial T}{\partial r}\right|_{r=R_a}=h_{tube1}[T_a(z)-T(z,R_a)] \qquad \text{For r =}R_a\ (2.3)$$

$$-k_{tube}\left.\frac{\partial T}{\partial r}\right|_{r=R_b}=h_{tube2}[T(z,R_b)-T_b(z)] \qquad \text{For r =}R_b\ (2.4)$$

For the intermediate air gap:

$$(\rho Cp)_{mair}\frac{\partial T}{\partial t}=k_{mair}\left[\frac{\partial^2 T}{\partial z^2}+\frac{1}{r}\left(\frac{\partial}{\partial r}\left(r\frac{\partial T}{\partial r}\right)\right)\right] \quad (3)$$

Boundary conditions:

$$-k_{mair}\left.\frac{\partial T}{\partial z}\right|_{z=L_a}=h_l[T(L_a,r)-T_l(r)] \qquad \text{For z =}L_a\ (3.1)$$

$$-k_{mair}\left.\frac{\partial T}{\partial z}\right|_{z=L_b}=h_u[T_u(r)-T(L_b,r)] \qquad \text{For z =}L_b\ (3.2)$$

$$-k_{mair}\left.\frac{\partial T}{\partial r}\right|_{r=R_a}=h_{mair1}[T_a(z)-T(z,R_a)] \qquad \text{For r =}R_a\ (3.3)$$

$$-k_{mair}\left.\frac{\partial T}{\partial r}\right|_{r=R_b}=h_{mair2}[T(z,R_b)-T_b(z)] \qquad \text{For r =}R_b\ (3.4)$$

For the electrical resistance layer:

$$(\rho Cp)_{heater}\frac{\partial T}{\partial t}=S+k_{heater}\left[\frac{\partial^2 T}{\partial z^2}+\frac{1}{r}\left(\frac{\partial}{\partial r}\left(r\frac{\partial T}{\partial r}\right)\right)\right] \quad (4)$$

Boundary conditions:

$$-k_{heater}\left.\frac{\partial T}{\partial z}\right|_{z=L_a}=h_l[T(L_a,r)-T_l(r)] \qquad \text{For z =}L_a\ (4.1)$$

$$-k_{heater}\left.\frac{\partial T}{\partial z}\right|_{z=L_b}=h_u[T_u(r)-T(L_b,r)] \qquad \text{For z =}L_b\ (4.2)$$

$$-k_{heater}\left.\frac{\partial T}{\partial r}\right|_{r=R_a}=h_{r1}[T_a(z)-T(z,R_a)] \qquad \text{For r =}R_a\ (4.3)$$

$$-k_{heater}\left.\frac{\partial T}{\partial r}\right|_{r=R_b}=h_{r2}[T(z,R_b)-T_b(z)] \qquad \text{For r =}R_b\ (4.4)$$

For the insulator:

$$(\rho Cp)_{mon}\frac{\partial T}{\partial t}=k_{mon}\left[\frac{\partial^2 T}{\partial z^2}+\frac{1}{r}\left(\frac{\partial}{\partial r}\left(r\frac{\partial T}{\partial r}\right)\right)\right] \quad (5)$$

Boundary conditions:

$$-k_{mon}\left.\frac{\partial T}{\partial z}\right|_{z=L_a}=h_l[T(L_a,r)-T_l(r)] \quad \text{For z =L}_a\ (5.1)$$

$$-k_{mon}\left.\frac{\partial T}{\partial z}\right|_{z=L_b}=h_u[T_u(r)-T(L_b,r)] \quad \text{For z =L}_b\ (5.2)$$

$$-k_{mon}\left.\frac{\partial T}{\partial r}\right|_{r=R_a}=h_{mon1}[T_a(z)-T(z,R_a)] \quad \text{For r =R}_a\ (5.3)$$

$$-k_{mon}\left.\frac{\partial T}{\partial r}\right|_{r=R_b}=h_{mon2}[T(z,R_a)-T_b(z)] \quad \text{For r =R}_b\ (5.4)$$

For the outer wall:

$$(\rho Cp)_{wall}\frac{\partial T}{\partial t}=k_{wall}\left[\frac{\partial^2 T}{\partial z^2}+\frac{1}{r}\left(\frac{\partial}{\partial r}\left(r\frac{\partial T}{\partial r}\right)\right)\right] \quad (6)$$

Boundary conditions:

$$-k_{wall}\left.\frac{\partial T}{\partial z}\right|_{z=L_a}=h_l[T(L_a,r)-T_l(r)] \quad \text{For z =L}_a\ (6.1)$$

$$-k_{wall}\left.\frac{\partial T}{\partial z}\right|_{z=L_b}=h_u[T_u(r)-T(L_b,r)] \quad \text{For z =L}_b\ (6.2)$$

$$-k_{wall}\left.\frac{\partial T}{\partial r}\right|_{r=R_a}=h_{wall1}[T_a(z)-T(z,R_a)] \quad \text{For r =R}_a\ (6.3)$$

$$-k_{wall}\left.\frac{\partial T}{\partial r}\right|_{r=R_b}=h_{wall2}[T(z,R_b)-T_b(z)] \quad \text{For r =R}_b\ (6.4)$$

T denotes the temperature (ºK), k the thermal conductivity (J/(s m ºK)), h the heat transfer coefficient (J/(s m^2 ºK)), S the electrical power per unit volume (J/(s m^3)), U_z the average velocity of the gas flow, r and z are the radial and axial coordinates respectively. The indices u and l correspond to the upper and lower boundaries of each section in the axial direction while a and b correspond to the boundaries between different layers in the radial direction. The modeling of each of the other four sections is constructed similarly.

Fig. 5 shows the dynamic response of the temperature in each layer of the third section of the reactor, during a process with a successive heating and cooling stage. Fig. 6 shows the variation of the catalyst and gas stream temperature along the axial position in the reactor. Fig. 7 shows the temperature of all layers in the third section along the radial direction, after 6 hours. The axial domain was discretized using second order backward finite differences over a uniform grid of five intervals. On the other hand, the radial domain was handled using orthogonal collocation on finite elements with third order polynomial approximation over one finite element. The model equations were solved in gPROMS [3] an integrated modeling environment.

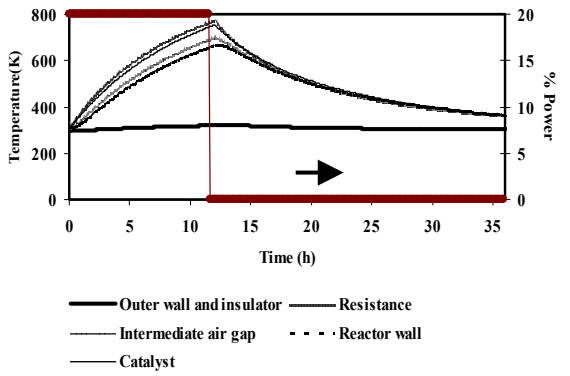

Fig.5 Temperature variation in all layers with successive heating and cooling operating conditions.

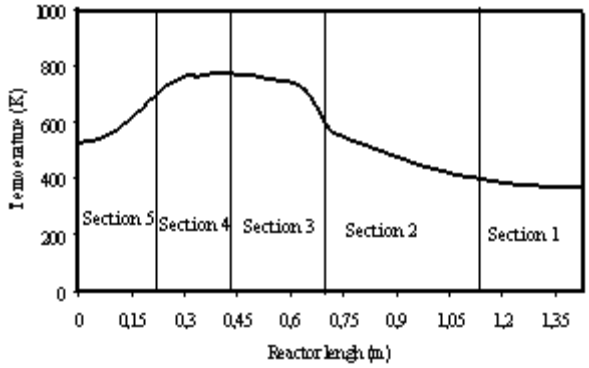

Fig. 6 Catalyst and gas stream temperature in axial direction at t = 6 h, r =0.0 m.

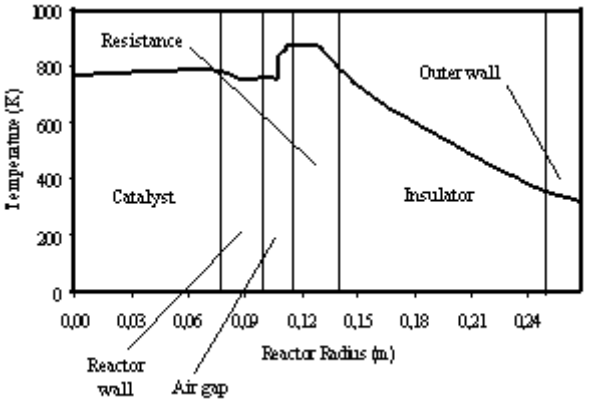

Fig.7 Temperature in all layers of the third section in radial direction at t = 6 h, z =0.302 m

IV. Parameter Estimation

The calculation of the optimal estimates for key model parameters is essential for the development of an accurate process model for control purposes. Frequent updates of the model parameters during operation are necessary as the operating conditions span a wide temperature range and reaction regimes. The selection of the estimated parameters was performed considering their influence in the dynamic response of the model and the availability of process measurements. The calculation of the parameter estimates was performed using the Maximum Likelihood method (ML) ([4], [5]).

The dynamic measured data were collected from three experiments with different initial and operating conditions. In the first experiment, the catalyst's section was heated with the 20% of the total power for 12 hrs and cooled for 24 hrs. In the second experiment, the catalyst's section was heated continuously for 52 hrs with the 10% of total power in the associated heating section. In the third experiment, all five reactor sections were heated with the 40% of their total power of each section's heater for 2.5 hrs and then cooled for 24 hrs. Afterwards they were heated again with the 30% of the total heater power for 2 hrs and finally cooled down for 22 hrs.

The measured variables were temperature values at different locations within the system as shown in Fig. 4. More specifically, the measurements include the catalyst's temperature at three different points (low, middle and upper point at the center of the third section), the tube's temperature at three points in the middle of the first, second and third sections and the bottom air's temperature at two points (one in the upper part of the fourth section and one in the middle part of the fifth section). The locations of the thermowells in the unit do not necessarily correspond exactly to the discretization points of the modeling equations. In order to tackle this problem the variables closer to the thermowell location were selected for the formulation of the parameter estimation problem. The variation of measurements was assumed constant and known.

The selected estimated parameters were: the thermal conductivities of the catalyst fluidized bed, the reactor wall, the resistance layer and the insulator (k_{cat}, k_{tube}, k_{heater}, k_{mon}) and the ρC_p of the refractory material, where the electrical resistances were embedded. The initial and estimated values of the parameters accompanied with the 95% confidence intervals and standard deviation are presented in Table 1.

Table 1

Parameters	Initial Value	Optimal Estimates	95% Confidence Interval	Standard Deviation
k_{cat}	3.54E+01	5.46E+01	5.99E-01	3.05E-01
k_{tube}	3.70E+02	2.55E+02	3.30E+00	1.68E+00
k_{heater}	9.00E-01	1.08E+00	1.99E-02	1.02E-02
k_{mon}	1.80E-01	1.01E-01	2.11E-03	1.08E-03
ρC_p	4.45E+06	4.50E+06	1.05E+04	5.38E+03

Fig. 8 shows the 95% joint confidence ellipsoids for the k_{cat} and k_{heater} and k_{mon} estimates. The ellipsoids show small correlation among estimates. Fig. 9-11 compare the experimental data with the model predictions in the three dynamic experiments. The agreement in the first two experiments is very good. In the third experiment an error of 10 % was observed at the peak temperature.

The observed discrepancies are attributed to the uncertainty of the exact position of the thermowells inside the reactor, the measurement random error and the assumption of constant parameter values (e.g. ρ, C_p and so forth) in relation to the operating conditions of the unit.

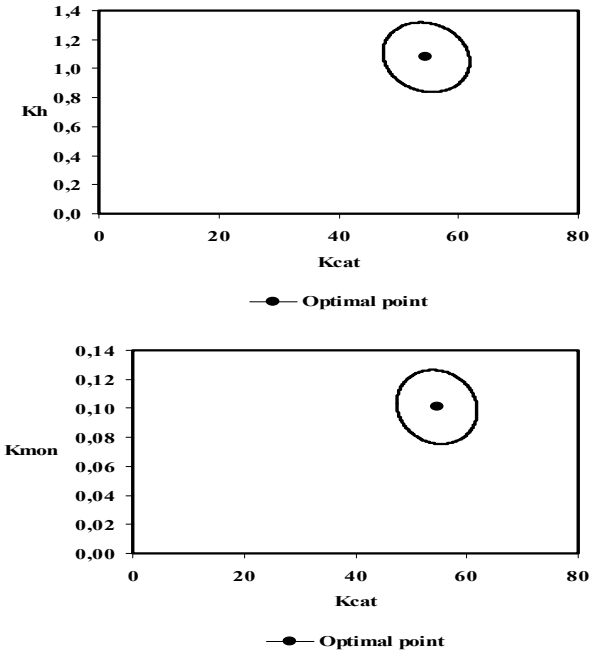

Fig. 8 Confidence ellipsoids 95%

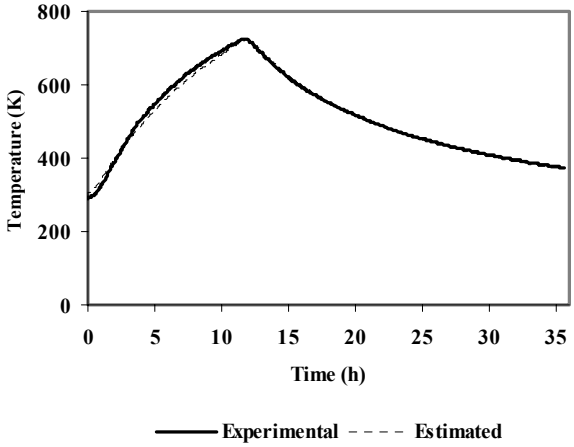

Fig. 9 Comparison between experimental and estimated data of the catalyst's temperature in the case of the first experiment's operating conditions.

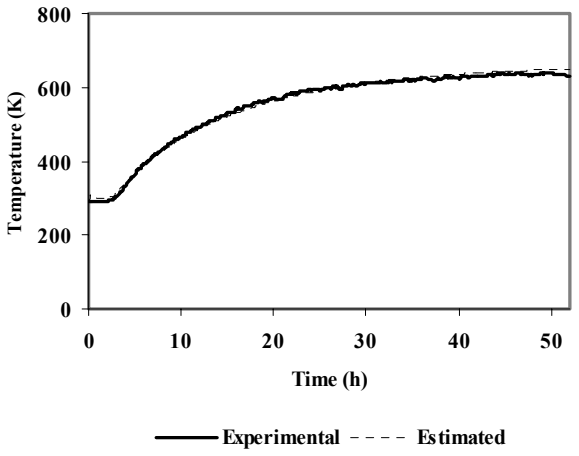

Fig. 10 Comparison between experimental and estimated data of the catalyst's temperature in the case of the second experiment's operating conditions.

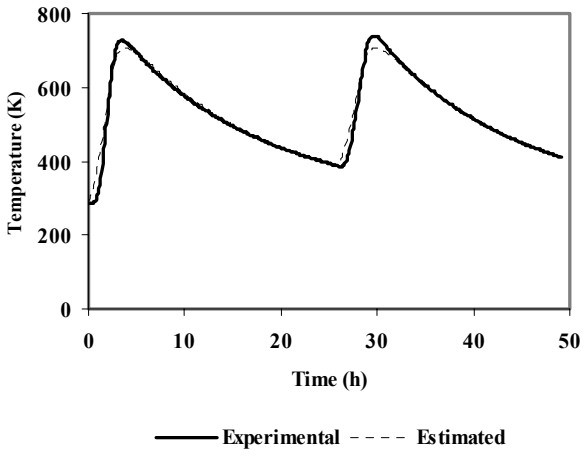

Fig. 11 Comparison between experimental and estimated data of the catalyst's temperature in the case of the third experiment's operating conditions.

V. CONCLUSIONS

A two-dimensional dynamic model of a fluidized bed reactor used for catalyst evaluation (CPS) was developed. Parameter estimation was performed using ML method and dynamic experimental data from the CPS unit.

The verified model will provide the base for the development of a model based optimal predictive control algorithm for the unit.

REFERENCES

[1] T.E. Marlin, "Process Control", McGraw Hill, N.Y., 1995.
[2] R.B. Bird, W.E. Stewart and E.N. Lightfoot, "Transport Phenomena", Wiley Int. Ed.,N.Y., 1960.
[3] Process Systems Enterprise, gPROMS, Version 2.33, User's Guide, 2004.
[4] W.J.H. Stortelder, "Parameter Estimation in Nonlinear Dynamical Systems", Ph. D Thesis, University of Amsterdam, 1998.
[5] D.P.Psoinos, "Statistics", Thessaloniki ,1978.